Excitation Spectra of the Impurity Anderson Model Calculated by the Numerical Renormalization Group Method

Osamu SAKAI, Yukihiro SHIMIZU and Tadao KASUYA

Department of Physics, Tohoku University, Sendai 980

(Received October 21, 1991)

A method to calculate the excitation spectra of the impurity Anderson model based on the numerical renormalization group technique is reviewed. The single particle and the magnetic excitation spectra are calculated for the cases of various magnitudes of the f-f Coulomb interaction to compare them with experimentally observed broad PES-BIS spectra in U-compounds. Excitation spectra in the Kondo limit are also examined in detail. The Kondo effect due to the magnetic ions with complex multiplet structures, such as the Sm- and the Tm-like ions, is studied. The excitation spectra of the two impurity Anderson model are calculated and roles of the parity splitting are discussed.

§ 1. Introduction

In this paper we review our recent calculation for the excitation spectra of the impurity Anderson model. The method of calculation is developed based on the numerical renormalization group (NRG) technique which has been originally introduced by Wilson to study the thermodynamic properties of the Kondo problem.[1),2)]

The purposes of the calculation are three folds. The first one is to study the single particle excitation (SPE) spectra of the impurity Anderson model in wide energy range.[3),4)] We study roles of the atomic f-f Coulomb interaction in the origin of the broad PES-BIS spectra of U-compounds, in which the atomic interactions and the c-f hybridization are expected to have comparable magnitude.

The second one is to study the dynamical excitation spectra of the Kondo problem. Several approximation schemes have been developed to study the dynamical properties of the problem, but exact excitation spectra at very low temperature have not been obtained before our calculation. We calculate the spectra of SPE, magnetic and charge excitations in the low energy region of the order of the Kondo temperature, T_K, carefully.[5)]

The third one is to study the Kondo effect due to the magnetic system with complex internal level structure, such as Sm and Tm ions,[6)] or the two magnetic impurity system.[7),8)] At present the numerical approach based on the NRG may be one of the best way to study such complex systems because the application of the analytic approach based on the Bethe Ansatz seems to be very difficult.

Method of calculation based on the NRG is explained in § 2, and each subject is discussed in the following sections.

§ 2. Method of calculation

In the NRG method,[1),2)] first the conduction band is discretized by the logarithmic mesh to give good sampling to states near the Fermi energy. Next it is transformed to an expression represented by the shell orbits. The orbits are arranged in an order spreading in space from the most localized orbit which hybridizes directly with the atomic f-orbit. They have hopping matrix between neighboring shell orbits.

Usually, the NRG method is applied to a model with constant hybridization matrix not dependent on band energy. However, it can be applied to a model with more general form of the hybridization matrix when one generates the shell orbits numerically by successive use of the commutation relation with the conduction band term.[9)] The Hamiltonian for the single impurity problem is given in the following form,

$$H=H_f+\sum_m V(f_m{}^+ s_{0m}+\text{h.c.})+\sum_{l=0}^{\infty}\sum_m\{t_l(s_{lm}^+ s_{l+1m}+\text{h.c.})+\varepsilon_l s_{lm}^+ s_{lm}\}\,, \tag{1}$$

where s_{lm} denotes the annihilation operator of the electron in the l-th shell orbit with symmetry m, f_m that of the atomic f-orbit. We assume that the f-orbit is classified by one angular momentum j neglecting the excited orbit of the spin-orbit interaction. The index m runs over from $-j$ to j and thus the degeneracy factor N is given by $2j+1$. The quantity V gives the strength of the c-f hybridization defined by the following expression: $V=(\int dE A_\Lambda M(E))^{1/2}$, where $M(E)=\sum_k|v_k(m)|^2\delta(E-\varepsilon_k)$ is the hybridization matrix, $v_k(m)$ the hybridization matrix element for the m-component and ε_k the band energy. The quantity, $A_\Lambda(\sim 1)$, is the correction factor for the discretization, which depends weakly on the discretization parameter $\Lambda(>1)$ and is defined in Ref. 2). We consider the case that $M(E)$ does not depend on m. The quantity t_l is the hopping matrix between the shell orbits and ε_l the energy level of the l-th shell orbit. When $M(E)$ has electron-hole symmetry: $M(E)=M(-E)$, ε_l becomes zero. It decreases as Λ^{-l} when l increases, while the hopping matrix usually tends to $D(1+\Lambda^{-1})\Lambda^{-l/2}/2$, which is the expression given by Krishna-murthy et al.[2)] for the constant hybridization with band ranges from $-D$ to D.

The term H_f gives atomic energy states of f-electron. Most general form which has rotational symmetry is given by the following expression,

$$H_f=\sum_{nJM}|f^nJM\rangle E(f^nJ)\langle f^nJM|\,, \tag{2}$$

where $|f^nJM\rangle$ denotes the atomic state with electron number n, the total angular momentum J, and the magnetic quantum number M. The quantity, $E(f^nJ)$ is the energy of the state. If we consider the usual Anderson model with constant f-f interaction, $E(f^nJ)$ is given as $n\varepsilon+Un(n-1)/2$. Here, ε is the energy level of f-orbit and U the Coulomb interaction constant. We choose the energy of atomic state more freely to study the effect of the multiplet splitting.

Following the method described in Refs. 2) and 3), we first diagonalize the H_f term. Next in the manifold of the product space of the eigenstates of H_f and the

$l=0$ shell states, the Hamiltonian including up to the $l=0$ shell orbit is diagonalized. Similarly by adding shell orbit successively, the total Hamiltonian is diagonalized step by step by the iterative method. Hereafter we denote by H_N the Hamiltonian including up to the N-th shell orbit. The matrix elements needed in this procedure are obtained in a compact form by using the $6j$ symbol.[10] When we actually do calculation, we discard high energy states and keep only a small number of low energy states to next iteration step because of the computational capacity. It is known that this truncation procedure does not cause serious effect on the low energy states since the hopping matrix decreases with l.[1]

At a given step of this iteration process, N, the lower energy states are expected to be good approximate states to the exact eigenstates of H_N which would be obtained without the truncation process. When we proceed the iteration step to $N+1$, the very low energy levels are affected by the interaction with the added shell states, but the intermediately low energy levels do not show any essential change because the interaction is small. Therefore, the latter states may be regarded as good approximate eigenstates of H_{N+1}, and thus of the Hamiltonian in the infinite N limit. We calculate the excitation energies and the transition matrices by using these states.[3] At this stage, however, the true ground state in the infinite N limit is not known. In this paper we have used the lowest energy state in this iteration step as the initial state of the transition. When we proceed the step, the energy region where the good approximate states are obtained shifts to low energy side successively. In practice, scaling of energy by the hopping matrix is convenient in numerical treatment. Therefore the same energy region in the scaled Hamiltonian is used to calculate the excitation spectra.

The calculated excitation spectra are given as the collection of the spikes because we use the discretized model. They are smoothed by the Gaussian shape function in the logarithmic energy scale,[3]

$$S(E)=\sum_e \frac{1}{\sqrt{\pi}\eta E_e}\exp\left\{-\left(\frac{\ln E/E_e}{\eta}\right)^2-\eta^2/4\right\}p_e\,. \tag{3}$$

Here e denotes the excited state, and E_e and p_e are the excitation energy and the transition probability, respectively. The quantity η is a factor of the order 1 which controls the width of the Gaussian. For a given step of iteration, N, we choose the energy E_N at which the excitation spectra are calculated as follows, $E_N=\zeta D\times(1+\Lambda^{-1})\Lambda^{-(N-1)/2}/2$ with a factor ζ of the order 1.

Optimal choice of η and ζ depends on the width of energy range where the energy states are reliable. We should choose ζ as large as possible if we can get enough reliable energy range. However, it is not necessary to take so much large value. In Fig. 1 we show the calculated spectra for several cases of η and ζ for $N=3$ model.[5] The circles give the data points of the SPE spectrum of f-electron (ρ_f), and the triangles and diamonds are those of the imaginary part of the magnetic (χ''_m) and the charge (χ''_c) susceptibilities of f-electron, respectively. Smooth curves are obtained when we join series of data points in only odd, or only even N steps. But they do not agree with each other in general. Due to this fact, the data points deviate from the

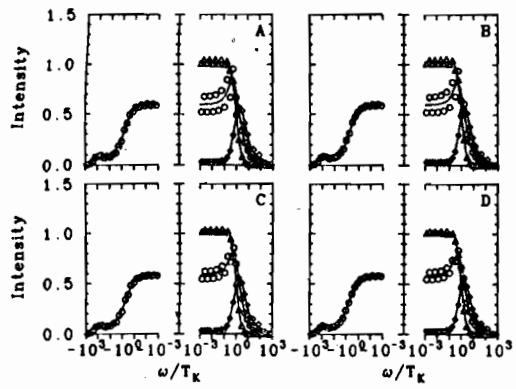

Fig. 1. Spectral intensities calculated by typical choice of η and ζ parameters. The circles give data points of the spectrum of the SPE ($\pi\Delta\rho_f(\omega)/N$), the triangles give the magnetic ($3T_K^2N\chi_m''(\omega)/\pi\omega j(j+1)$), and the diamonds the charge ($\chi_c''(\omega)/2\pi\omega N$) excitations. The abscissa is the energy in the logarithmic scale, the negative energy side represents the hole excitation (PES part) and the positive side the electron excitation (BIS part). $\eta=0.45\ln\Lambda$ for A and B, and $0.52\ln\Lambda$ for C and D and $\zeta=5.4$ for A and C, and $5.4\,\Lambda^{-1/2}$ for B and D. The lines are obtained by the procedure explained in the text. Parameters are $N=3$, D (half of the band width)$=1$, $\varepsilon=-0.3$, $U=10$ and $M=0.02$, and the quantity Δ is the hybridization width, πM. The number of states kept to next iteration step, N_{cut}, is about 1600 and $\Lambda=3$. $T_K=2.91\times10^{-3}$ and Wilson's ratio is 1.5.

lines in the figure. The lines are obtained by averaging the two curves which are calculated using the spline interpolation for each series of data.

As seen from Fig. 1, the averaged line does not depend on choice of η and ζ so seriously. In the present calculation, the lowest energy state in each step is used as the initial state of transition. This seems to be over simplification. If the transition probabilities are averaged over several initial states, the scattering of data point of odd and even steps will be removed. Actual calculations by using this procedure are remained in future problems. Another averaging methods of data have been proposed by Brazilian group.[11),12)] Averaging of curves obtained from the even and odd steps seems to work as the averaging of initial states.

The integrated intensity of the PES spectrum is normalized to give n/N, where n is the total occupation number of f-electron. We get $n=0.871$ from A and 0.855, 0.858, 0.853, from B, C and D, respectively, by the numerical integration. On the other hand we obtain $n=0.881$ from the expectation value in the ground state. The density of states at the Fermi energy is also expected to be 0.635 from the rigorous Fermi liquid relation,[13)] while that is estimated as follows 0.595, 0.595, 0.583 and 0.582, from Figs. 1. Using the values $-\chi_m''(E)/E(E\to0)$ estimated from the lines, we get the following values for the static susceptibility 2.35×10^2, 2.36×10^2, 2.36×10^2 and 2.33×10^2 by using Korringa-Shiba's relation.[14)] On the other hand we obtain 2.24×10^2, 2.26×10^2, 2.20×10^2 and 2.18×10^2 based on the Kramers-Kronig relation. The susceptibility is also estimated to be 2.29×10^2 from the effective Hamiltonian approach near the low energy fixed point.[2)] These results indicate that the present calculation shows rather good consistency not so much depending on the choice of η and ζ. We use $\eta=0.52\ln\Lambda$ and $\zeta=5.4$ hereafter for $\Lambda=3$ and $\eta=0.64\ln\Lambda$ and $\zeta=1.7$ for $\Lambda=2$ because the curves of odd and even series do not so much deviate from each other. We note, however, that the averaged line shows good consistency rather in cases with large deviation of even and odd curves, for example Fig. 1A.

§ 3. Excitation spectra for the cases of various magnitudes of the f-f Coulomb interaction

In Fig. 2 we show excitation spectra for $N=4$ and constant f-f interaction model for various cases of ϵ and U.[3] Figures 2 (A, E, I, M) give spectra in the electron-hole symmetric case. The main peak at the Fermi energy of the SPE becomes narrow as U increases, and tends to the Kondo resonance. At the same time the tails of it grow gradually to broad shoulders of the Kondo resonance, and they split off as the peaks corresponding to the $f^2 \to f^1$ and $f^2 \to f^3$ excitation. The peak height is about 89% of the value expected from the Fermi liquid relation, thus accuracy of the present calculation will be enough for qualitative discussions.

Figures 2 (B, F, J, N) are the spectra when the atomic energy levels of f^1 and f^2 are degenerate. The width of the peak at the Fermi energy does not decrease so drastically compared with the symmetric case when U increases. Even in this case the intensity of the charge fluctuation does not increase and its energy scale seems to be of the order of the hybridization width. The SPE spectrum has tails with energy scale of the charge fluctuation. The tail in the BIS side is larger because the multiplicity factor is larger in the electron excitation.

When the occupation number of the f-electron has values a little larger than the integer, we have a broad shoulder in BIS side of the main peak as seen from Figs. 2 (C, G, K, O). In the case that the occupation number has almost integral value, 1, general features are similar to the cases (C, G, K, O). The broad shoulder in BIS gradually splits off as the $f^1 \to f^2$ atomic excitation when U increases. Weak peak of $f^1 \to f^0$ excitation also appears in PES side. This type of spectrum corresponds to the Ce ion case.[15] When the occupation number decreases further to smaller value than 1, the effect of the Coulomb interaction becomes less important as shown in Ref. 3).

The magnetic excitation has energy scale comparable to the width of the main peak of the SPE spectrum at the Fermi energy. The width of the main peak is always smaller than that of the non-interacting case as seen here and in Ref. 3). This may indicate in some sense that the f-band width will be always narrowed by the f-f Coulomb interaction.

The SPE spectrum of U-compounds has broad peak in the BIS side.[16)~19)] Its width is larger than that of the band calculation,[20)] while the low energy excitation, such as the magnetic excitation, has smaller energy scale.[17)] One possibility to interpret the experimental facts may be to assign the broad BIS structure to the broad shoulder appearing in relatively large U cases. As discussed in Ref. 3), U should be larger than 8Δ to cause the broad shoulder in the $N=6$ case corresponding to U ion, where Δ is the hybridization width πM. In this interpretation the sharp peak should exist at the Fermi energy. It has not been observed at present, though there is a possibility that its sign has been observed in the high resolution PES experiment.[21)]

Usually, the hybridization in U-compounds is expected to be larger than Ce,[22)] and thus the width of the sharp peak will be much larger. It seems curious why the peak has not been observed in experiments. One possible origin of this discrepancy is the multiplet splitting of the atomic state.[4)] When the lowest energy configuration has multiplet splitting, the width of the Kondo resonance of the SPE and the energy scale

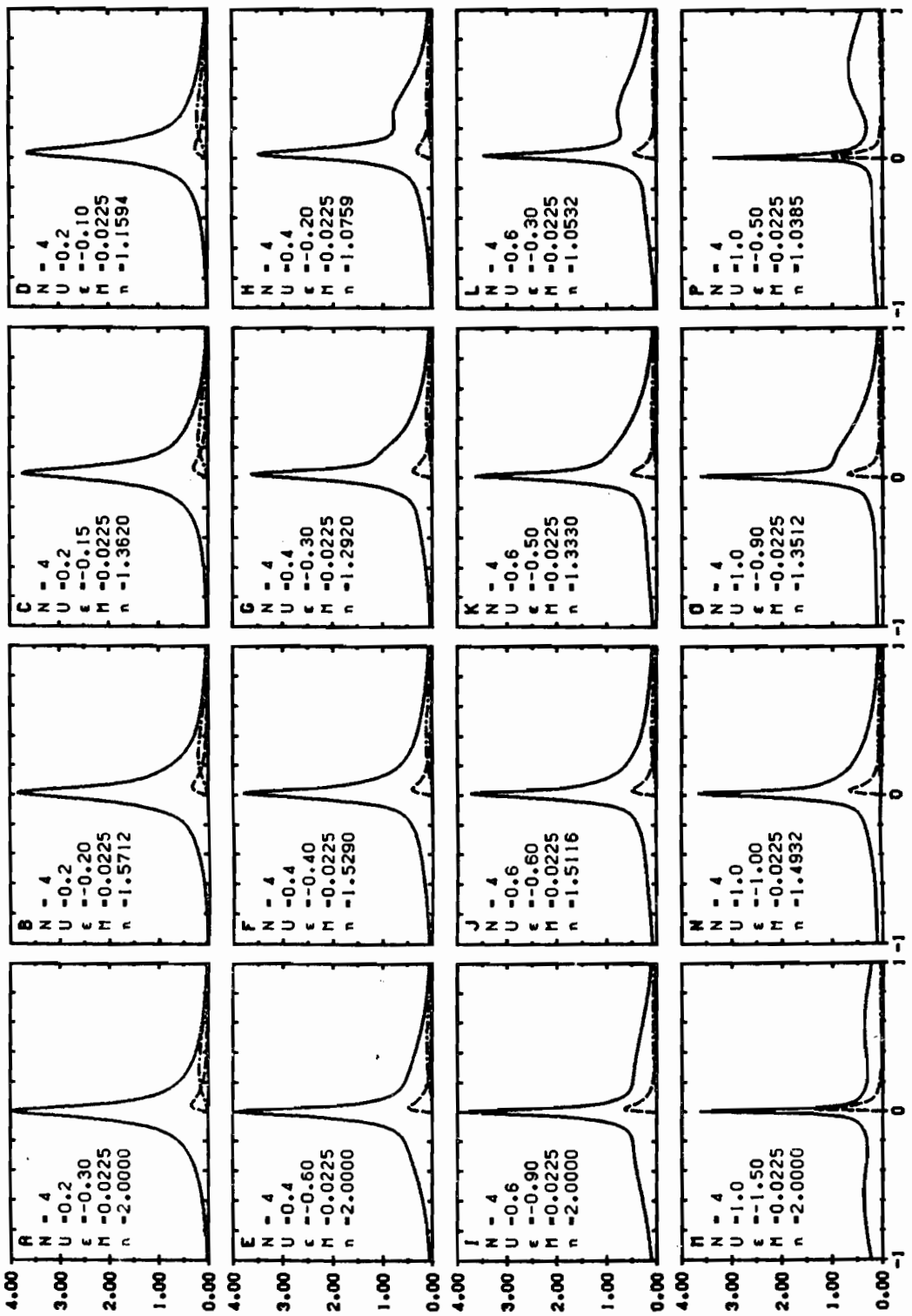

Fig. 2. Spectral intensities of the $N=4$ model in various parameter cases. The solid line is ρ_f/N, the dotted line $0.5\times\chi''_m/N$ and the dot-dashed line χ''_c/N. $D=1$, $N_{cut}\sim 600$ and $\Lambda=2$. The quantity n is the occupation number of f-electron.

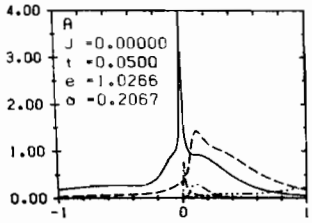

Fig. 3. Spectral intensities of the two channel model. The solid (dashed) line gives the SPE spectrum for the component with smaller (larger) hybridization M_e=0.02 (M_o=0.03) and lower (higher) energy level ε_e=−0.65 (ε_o =−0.55), $e(o)$ gives the occupation number of the $e(o)$ channel, $t=(\varepsilon_o-\varepsilon_e)/2$. D=1 and U =0.8. The dot-dashed line is the magnetic excitation of the intra-channel excitation and the dashed line the inter-channel excitation. $N_{cut}\sim$600 and Λ=2.

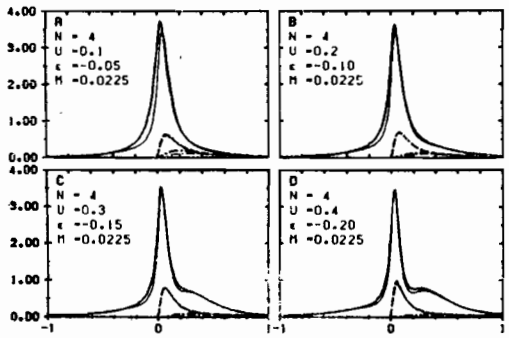

Fig. 4. Spectral intensities calculated by restricting atomic states to low energy configurations (f^0, f^1 and f^2). The thin lines are calculated by restricting states and the bold lines are by not restricting states. The solid lines give ρ_f, the dashed lines χ_m'' and the dot-dashed lines χ_c''. The bold and thin lines almost coincide in the χ_m'' and χ_c'' cases. The occupation number of f-electron is A) 1.30(0.93), B) 1.16(0.96), C) 1.10(0.98) and D) 1.08(0.99), where numbers in parentheses are for restricted cases. D=1, $N_{cut}\sim$600 and Λ=2.

of the magnetic excitation drastically decrease because the effective hybridization is reduced. Even in this case the effective hybridization for high energy processes is not reduced. Broad shoulder structure appears, which is a complex of the inter- and the intra- configurational excitations. To demonstrate excitation spectra in a similar situation in Fig. 3 we used a two channel model: One channel has smaller hybridization and lower atomic energy level than those of the other channel. The former gives sharp Kondo resonance and the main intensity of the PES part, while the latter gives main intensity of the BIS part. The integrated intensity of the Kondo resonance is very small and its width is comparable to the magnetic excitation energy. The structures at about 0.1 on both sides of the Fermi energy are mainly ascribed to the excitation between two channels (intra-configuration). The broad shoulder above 0.3 in BIS part is mainly due to the $f^1\rightarrow f^2$ excitation (inter-configuration).

Another possibility of the origin of the discrepancy between experiments and calculated results may be the simplification to the single site model. However as seen in the later section concerning to the two site model, we should, in principle, have in the SPE spectrum a structure corresponding to the low energy excitation modes even when they are not local. The intensity will be small if the q-dependence of the mode is large. It may be important to check whether both of the high[23),24)] and the low[25)] energy phenomena can be interpreted by the single impurity model, for example, by alloying or some other methods.

In Fig. 4, we show excitation spectra calculated by restricting the atomic states to low energy configurations. The thin lines are obtained by dropping configurations except the lowest (f^1) and other two low energy ones (f^0 and f^2). The bold lines are obtained by correct calculation. The high energy configurations can be neglected

when the effect of the Coulomb interaction becomes noticeable, $U>4\Delta$. It seems desirable to apply various theoretical methods[26)~28)] developed for the $4f$-systems based on the fact, $U\gg\Delta$, also to the $5f$-systems.

§ 4. Excitation spectra in low energy region

The exact solution based on the Bethe Ansatz,[29)] and the Fermi liquid approach[30)] usually treat only the thermodynamic properties or the very low energy properties. Several approximate methods have been developed to study the dynamical properties of the Kondo problem.[31)] However exact calculation of the excitation spectra has been left even for the s-d Hamiltonian. The NRG method was initially developed to study the thermodynamic properties and gave full picture of the cross over from the magnetic to the singlet state for the first time.[1)] In this section we show recent results for the calculation of excitation spectra in low energy region.[5)] This has been done more carefully for quantitative accuracy than the previous section.

In Fig. 5, we show the excitation spectra for $N=2$ model in various parameter cases.[5)] The solid line gives the SPE spectrum normalized by the hybridization width: $\rho_f(E)/((\pi\Delta)^{-1})$, the dashed line: $\chi_c''(E)/E$, and the dot-dashed line: $\chi_m''(E)/E$. The Kondo temperature is defined through the relation $\chi_m(T=0)=j(j+1)/3T_K$. The

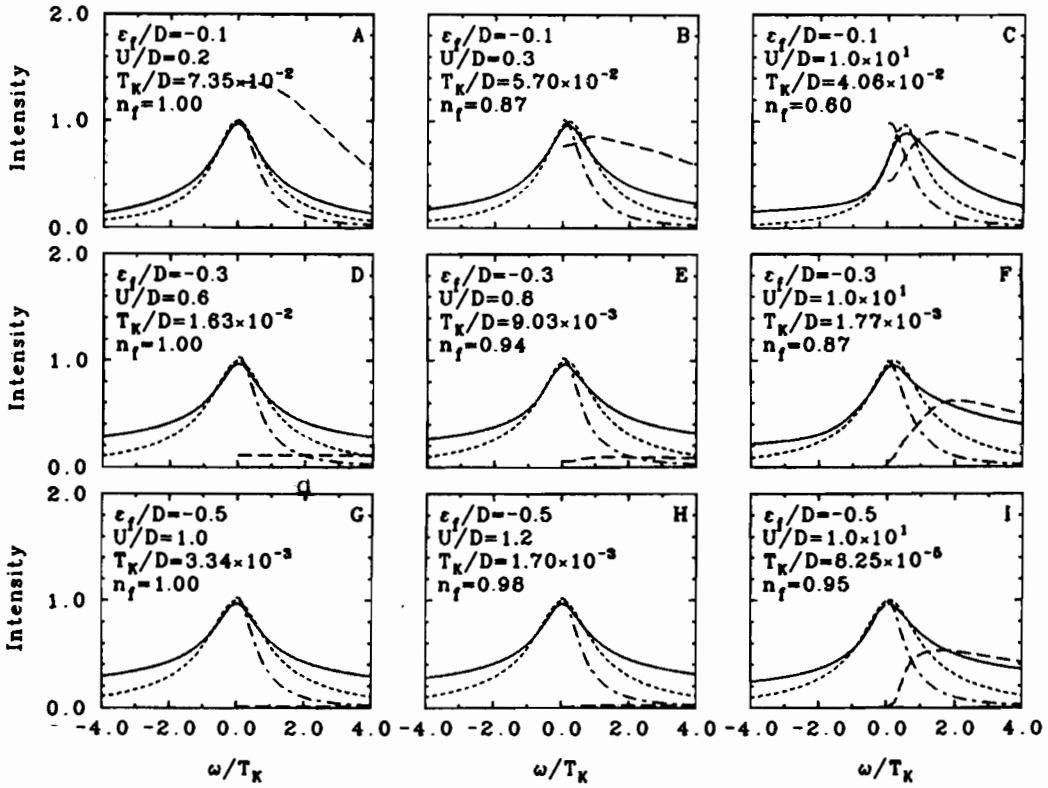

Fig. 5. Spectral intensities of $N=2$ model in low energy region. The solid line gives $\pi\Delta\rho_f/N$, the dot-dashed line $3T_K^2N\chi_m''/\pi\omega j(j+1)$ and the dashed line $\chi_c''/2\pi\omega N$. The dotted line is calculated by the 2nd order perturbation theory for ρ_f, see the text. $D=1$, $M=0.03$, $N_{cut}\sim1000$ and $\Lambda=2$. In this figure ε and n are written as ε_f and n_f.

dotted line is an approximate SPE spectrum drawn by using the second order perturbational expression for the self energy, where the hybridization width and the Coulomb interaction constant are replaced by effective ones of the effective Hamiltonian for the low energy fixed point.[5]

In the first row, A→C, the atomic excitation energy of $f^1 \to f^0$, ε, is kept constant and that of $f^1 \to f^2$, $\varepsilon + U$, is increased. In the lower rows, $|\varepsilon|$ is chosen to be larger. The columns A, D and G correspond to the electron-hole symmetric case, and the Coulomb interaction increases from A to G. The peak height of the SPE spectrum should be unity from the Fermi liquid relation. When U is much larger than the hybridization width Δ, the SPE spectrum tends to a universal shape when the energy is scaled by T_K as seen from D and G.

When the excitation energy of $f^1 \to f^2$ increases, the peak position of the SPE spectrum shifts to high energy side. At the same time it becomes gradually asymmetric with larger intensity in the high energy side. In the peak region, the spectrum calculated by the NRG is reproduced rather well by the dotted line given by the 2nd order perturbational theory, but has larger intensity in the tail region. The dotted line has almost Lorentzian shape with width about $1.3\,T_K$(HWHM). The intensity of the tail parts increases with U in smaller U region. But the line shape tends to a certain form in the large U limit when the occupation number of f-electron is fixed and energy is scaled by T_K.

The spectrum of the magnetic excitation seems to be scaled by T_K in the large U case. It fulfills Korringa-Shiba's relation.[14] The quantity $\chi_m''(E)/E$ has almost Lorentzian shape with width about $0.67\,T_K$(HWHM) in the $n \sim 1$ case. We note that $\chi_m''(E)$ is reproduced very well by the RPA-like expression in which the hybridization and the Coulomb interaction are replaced by effective ones determined from the

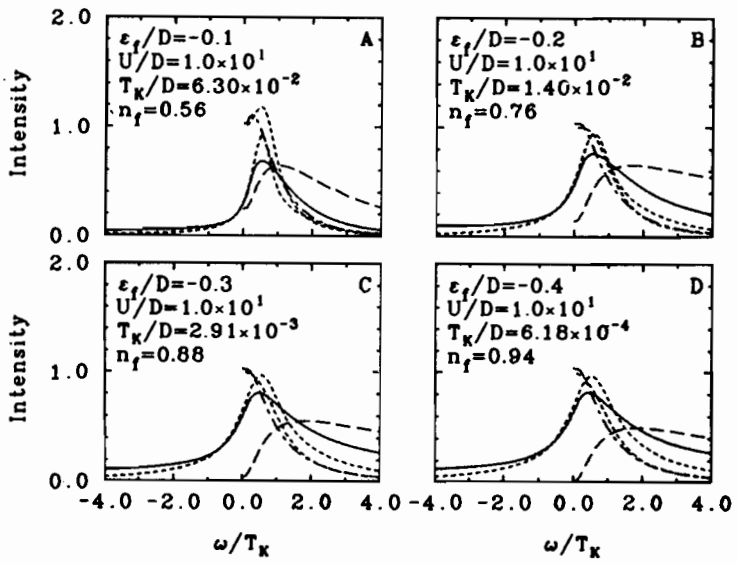

Fig. 6. Spectral intensities of the $N=3$ model in low energy region. See the caption of Fig. 5. The dotted line which shows similar behavior to χ_m''/ω is calculated by a RPA-like expression, see the text. $D=1$, $M=0.02$, $N_{cut} \sim 1600$ and $\Lambda=3$.

analysis of the low energy fixed point, $\Delta_{eff}\sim 1.3T_K$ and $U_{eff}\sim 4.0T_K$ in the $n\sim 1$ case.[5),32)]

The charge fluctuation is rapidly depressed as U increases. The quantity $\chi_c''(E)/E$ shows a peak structure at about $2T_K$ when the electron-hole asymmetry becomes large. But the intensity is very small.

In Fig. 6, we show excitation spectra in the case $N=3$ model.[5)] Present calculation gives about 94% of the value expected from the Fermi liquid relation for the spectral intensity of SPE at the Fermi energy. At a first glance, it has a shape similar to that of the $N=2$ model if the averaged occupation number, n/N, is the same. But in detail, the tail of BIS side is lager in $N=3$ case as seen from Figs. 5C and 6C. The spectrum of $\chi_m''(E)/E$ has larger width than that of the $N=2$ case. The peak position of it changes from $E=0$ point to finite E when n decreases. Deviation of the dotted line calculated from the RPA-like expression becomes noticeable in small n cases. In the Coqblin-Schrieffer model case ($n\sim 1$) of the $N=3$ model, the RPA-like expression is not bad as seen from Fig. 6D.

§ 5. Kondo effect for ions with complex energy level structure

Kondo behavior is observed in some dilute alloys containing Sm impurity, for instance $La_{1-x}Sm_xSn_3$.[33)] The Sm ion fluctuates mainly between $4f^5(Sm^{3+})$ and $4f^6$ (Sm^{2+}), and is primarily in the Sm^{3+} configuration. The ground state of the Sm^{3+} ($^6H_{5/2}$) ion has total angular momentum $J=5/2$. In Sm^{2+} ion, the ground state is the singlet ($^7F_0$), but the first excited state ($^7F_1$) with $J=1$ is located very near the ground state, at about 400 K above. Thus the fluctuation between the magnetic states occurs in addition to the fluctuation between the magnetic and the singlet states. Kondo effect due to the fluctuation between magnetic states is expected in Tm ion.[34)]

In this section we first study the Kondo effect for the model with a Sm-like multiplet structure.[6)] We consider a model with $j=3/2$, smaller than the actual value $j=5/2$ because of the computational capacity. The energies of atomic states $E(f^nJ)$ are chosen to simulate the multiplet structure of Sm ion. We select the magnetic state $f^1(J=3/2)$, the singlet state $f^2(J=0)$ and the magnetic state $f^2(J=2)$, and exclude other states. These may correspond to the $f^5(J=5/2)$, $f^6(J=0)$ and $f^6(J=1)$ states of Sm ion, respectively.

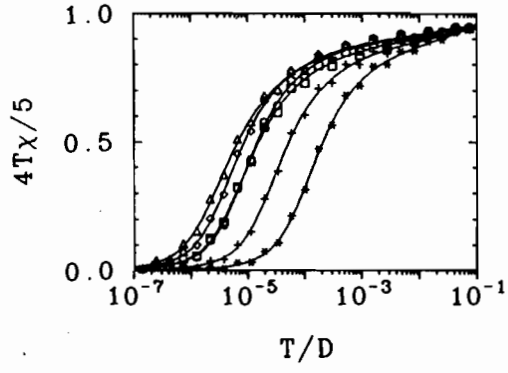

Fig. 7. Temperature dependence of the magnetic susceptibility in Sm-like systems, for $\Delta E=10(\bigcirc)$, $2(\diamond)$, $0.8(\triangle)$, $0.4(\square)$, $0.2(+)$ and $0.04(*)$. The other parameters are $D=1$, $M=0.015$, $E(f^13/2)=-0.3$, $E(f^20)=0$ and $\Delta E\equiv E(f^22)-E(f^20)$, energy levels of other atomic states are chosen to be 10, $N_{cut}\sim 1200$, $\Lambda=3$. χ_m is written as χ.

In Fig. 7, we show the temperature dependence of the magnetic susceptibility for various values of the multiplet energy difference, $\Delta E=E(f^22)-E(f^20)$.[6)] At very low temperature the ground state becomes always singlet. The temperature at which $T\chi_m$ decreases to a small value does not show monotonic

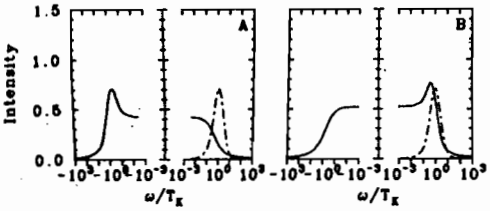

Fig. 8. Spectral intensities of Sm-like systems. The electron binding type (A, $\Delta E=2.0$, $T_K=1.19\times10^{-5}$) and the hole binding type (B, $\Delta E=0.2$, $T_K=7.25\times10^{-5}$) are shown. The solid line is $\pi\Delta\rho_f/4$, and the dot-dashed line $(16/5)T_K\chi_m''/\pi$. Parameters not indicated are the same as Fig. 7.

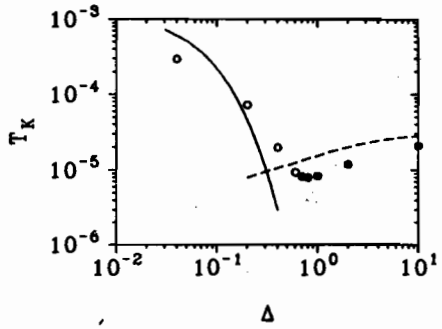

Fig. 9. Kondo temperature vs ΔE in Sm-like systems for the same parameters in Fig. 7. T_K is defined as $T_K=5/(4\chi(T=0))$. For solid and dashed lines, see the text. The filled circles indicate that the ground state is the electron binding type and the open circles the hole binding type. Parameters not indicated are the same as Fig. 7. ΔE is written as Δ in this figure.

change as ΔE changes. It falls when ΔE decreases from 10 to 0.6, but rises when ΔE decreases further from 0.6 to 0.04. By analyzing the level structure in the fixed point of low energy, we can see that an electron is bound in the same way as the Kondo state in Yb impurity case when ΔE is large. On the other hand a hole is bound in the same way as that in Ce ion when ΔE is small. This change of nature is also seen from the SPE spectrum shown in Fig. 8. The peak of the Kondo resonance appears in the PES side when ΔE is large, while it appears in the BIS side in the same way as that in Ce case when ΔE is small.

In Fig. 9, we show the Kondo temperature estimated from the susceptibility as a function of ΔE.[6] It becomes lowest in the region where the system changes from the electron to the hole binding type. The dashed line is the binding energy calculated by a variational wave function of the type: $f^2(0)\rightleftarrows f^1(3/2)+\text{electron}(j=3/2)$. It decreases as ΔE decreases because the effective excitation energy $f^1(3/2)\rightarrow f^2(0)$ increases due to the energy gain from the hybridization $f^1(3/2)\rightarrow f^2(2)$. The solid line is calculated by using a singlet variational function of the type: $f^1(3/2)+\text{hole}$ $(j=3/2)$.[34] The binding energy increases as ΔE decreases because the exchange coupling *via* the $f^2(2)$ state becomes strong.[28]

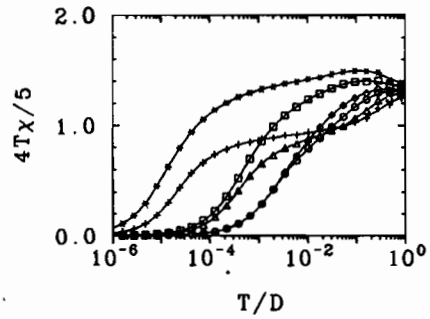

Fig. 10. Temperature dependence of the magnetic susceptibility of Tm-like systems for $E(f^2 2)=0.04(\bigcirc)$, $-0.04(\diamond)$, $0.2(\triangle)$, $-0.2(\square)$, $0.4(+)$ and $-0.4(*)$, respectively. The energy level $E(f^3 3/2)$ is 0, and those of other atomic states are chosen to be 10. $M=0.015$, $N_{cut}\sim1200$ and $\Lambda=3$. χ_m is written as χ.

We have estimated the Kondo temperature of Sm ion based on the variational wave functions by using the actual atomic multiplet structure. Usu-

ally the hole binding type state has higher T_K. This may explain the experimental result of a thermopower in $La_{1-x}Sm_xSn_3$, which shows positive sign similar to the Ce impurity type.[33]

Next we consider a case of fluctuation between the magnetic states f^3 ($J=3/2$) and f^2 ($J=2$). These may simulate the f^{13} ($J=7/2$) and f^{12} ($J=6$) states of Tm ion, respectively.[34] In Fig. 10, we show $T\chi_m$ for various cases of energy difference between $f^3(3/2)$ and $f^2(2)$ states.[6] At very low temperature, the ground state is always singlet. The Kondo temperature becomes highest when energies of the two states are nearly degenerate. By analyzing the level structure of low energy fixed point, we can see that the singlet state is constructed as $f^3(3/2)$+electron ($j=3/2$) when the energy of $f^3(3/2)$ state is lower, though the atomic state f^4 ($J=0$) has very high energy. The situation is essentially the same as in the small ΔE case of Sm ion. When the energy of $f_i^2(2)$ is lower, the singlet state is constructed as $f^2(2)$+electron^2 ($J=2$). In $n=2.44$ case, first the one electron bound state of the quartet type: $f^2(2)$+electron ($j=3/2$) becomes the lowest state, and then the two electron bound state becomes the lowest as the iteration step increases. However, this feature cannot be seen in $T\chi_m$ curve because the quartet region is very small.

§ 6. Two impurity problem

The problem of two magnetic impurities in a metal is extensively restudied recently as the starting point to understand interplay between the Kondo effect and the inter-site interactions, such as the exchange coupling between the local spins.[8),35] Jones et al. have pointed out that the γ-coefficient of the specific heat, γ, and the antiferromagnetic susceptibility of local spins diverge when the antiferromagnetic coupling between the spin pair has a critical value which separates the Kondo singlet like and the local-spin-singlet like states.[36] Recently the authors have calculated excitation spectra of the two impurity Anderson model and shown that the critical transition is suppressed when the f-electron occupation number shows parity splitting.[7] The critical transition is an artifact in the strict sense because the parity splitting is always induced from various sources, such as the f-f transfer or the parity dependence of the c-f hybridization. However, there is a possibility that the heavy fermion behavior has some relations to the critical transition, since it is usually accompanied with the magnetic instability.[37]

In Fig. 11,[8] we show excitation spectra for the model in which the f-f transfer and the parity dependence of the c-f hybridization are dropped in the same way as Jones et al. did. The indirect RKKY interaction is not induced in this case. We introduce exchange coupling between local spins as $J\sigma_1\sigma_2$, and use the hybridization matrix that is constant from -1 to 1, and zero outside of it. The SPE spectrum of f-electron and the imaginary part of the susceptibilities of the ferromagnetic moment (χ''), the antiferromagnetic moment (χ_a'') and the singlet non-uniform superconductivity (χ_s'')[38] are plotted.

The $J=0$ case corresponds to the independent single impurity model, and thus spectra of χ'' and χ_a'' coincide as seen from Fig. 11B. The Kondo temperature is estimated to be 7.68×10^{-3} from this calculation. The spectral intensity of the SPE at

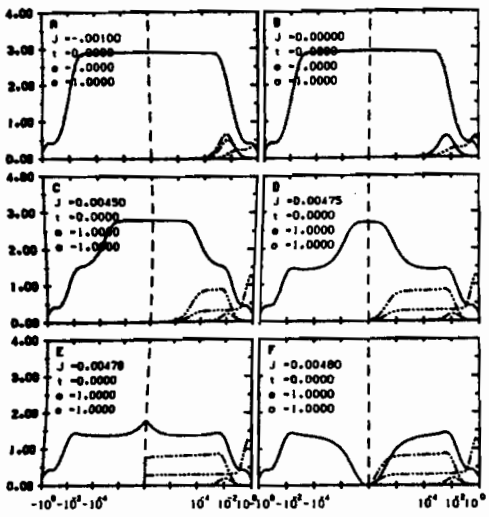

Fig. 11. Spectral intensities of the two impurity model without parity splitting terms. Hybridization matrix is constant in energy, 0.03, common to two channels, and $D=1$, $\varepsilon=-0.4$ and $U=0.8$. The quantity $e(o)$ denotes the occupation number of f-electron with even (odd) parity component, t the f-f transfer matrix. The solid line is the SPE spectrum, the dot-dashed line χ'', the two-dot-dashed line χ_a'' and the three-dot-dashed line χ_s''. One-fourth of χ'' and χ_a'', twice of χ_s'' are plotted. The abscissa is the energy in logarithmic scale in units of D. $N_{cut}\sim 600$ and $\Lambda=3$.

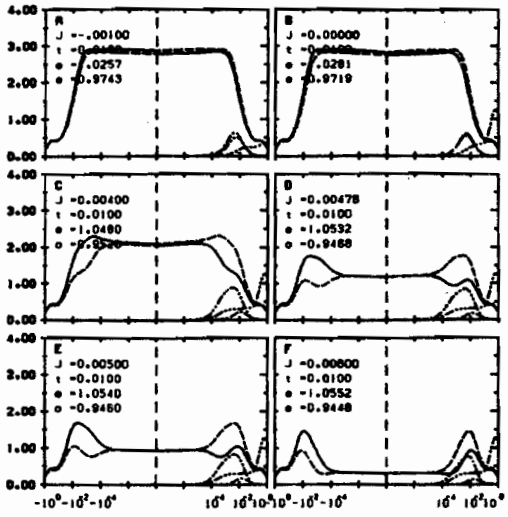

Fig. 12. Spectral intensities of the two impurity model with f-f transfer term, $t=0.01$. The solid (dashed) line gives the SPE spectrum of the even (odd) parity component. Parameters not indicated are the same as Fig. 11.

the Fermi energy is about 86% of the correct calculation for the single impurity problem.

Positive J means antiferromagnetic coupling between local spins. In the weak antiferromagnetic case, the low energy edge of χ_a'' shifts to low energy side at first, and peak of χ'' shifts to high energy slightly and its intensity decreases. The high energy edge of χ_a'' coincides with the energy of the peak position of χ'', thus corresponds to the freeze out of the free spin state. The SPE spectrum shows double structures, each corresponding to the low and high energy edges of χ_a''.

When J approaches to the critical value J_c which is estimated to be $j_c\equiv 4J_c/T_K\sim 2.49$ in the present calculation,[8] the low energy edge of χ_a'' seems to shift unlimitedly to zero. When J increases beyond J_c, the low energy edge begins to return to high energy. The energy corresponding to the low energy edge decreases as $(j-j_c)^2$ near the critical point, where $j\equiv 4J/T_K$.[8] From the analysis of energy levels in the low energy fixed point, we can see that γ diverges as $(j-j_c)^{-2}$.

The spectral intensity of the SPE at the Fermi energy remains constant when $J<J_c$, and it suddenly changes to zero when J goes over J_c. When J increases further to larger value, the spectral intensity of χ'' becomes very small, and χ_a'' shows a peak at energy comparable to J.

The height of the spectral intensity of χ_a'' is almost constant in the energy range between the low and high energy edges. This may relate to the origin of the diffusive component of the magnetic fluctuation in experiments.[37] The height almost does not change when J is in the antiferromagnetic region. The static susceptibility of the antiferromagnetic moment, χ_a' diverges at j_c as $-\ln|j-j_c|$. The susceptibility of the superconductivity shows similar behavior to that of χ_a'', but its intensity is about 1/10 of the latter.

In Fig. 12, we show excitation spectra in the case that the f-f transfer, t, is chosen to be comparable to the Kondo temperature for the single impurity problem.[8] When J is small, the Kondo peak of the SPE shows small parity splitting. When J increases near to J_c, the electron-hole asymmetry in each parity channel becomes noticeable. The even (odd) component shows a larger peak below (above) the Fermi energy and a smaller one above (below) the Fermi energy. The peaks have structures corresponding to the low and high energy edges of χ_a''. The spectral intensity at the Fermi energy decreases gradually as J increases, and does not show the sudden change.

The softening of χ_a'' is bounded as seen from Fig. 12C. Effective exchange interaction between local spins is modified because the f-f transfer term induces the kinetic exchange coupling which is estimated to be t^2/U in the lowest perturbation theory. So we have swept some range of J near J_c, but cannot find sign of the softening to zero energy.

The γ-coefficient is given as $\gamma\sim(T_K/t)^2$, and $\chi_a'\sim\ln T_K/t$ at $J=J_c$. More strictly, the low energy scale of the two impurity problem, ω_l, is approximately given as $\omega_l \sim T_K\{((j-j_c)/1.5)^2+(t/23T_K)^2\}$ near the critical point.[8]

When the f-f transfer matrix increases, the parity splitting of the SPE spectrum increases. We have calculated the parity splitting of f-level in the effective Anderson model which reproduces the energy level structures near the low energy fixed point. The effective transfer matrix, t_{eff}, is given as $t_{eff}\simeq t/Z$, when t is very small (less than $5T_K$) and the total effective exchange coupling between local spins ($J_{eff}=J+t^2/U$) is also very small. Here, the quantity Z is the enhancement factor of the specific heat of the single impurity problem.[39] In this parameter region, the physical properties seem to be dominated by single impurity character. When t increases beyond $5T_K$, the parity splitting increases and γ decreases drastically. This destruction of the Kondo state is mainly caused by the antiferromagnetic coupling induced by t. If we choose $J_{eff}=0$, the effective parity splitting remains to be order of t/Z. This may indicate that estimation of the reduction factor of f-band width by using the factor Z^{-1} is not so bad[40),41] when the inter-site magnetic coupling is not large. But when the magnetic fluctuation is strong, an approach treating explicitly the coupling with the magnetic excitation seems to be necessary.[32),42]

We have also examined the effect of the parity dependence of the c-f hybridization. General features of the spectra are similar to those in the case where the parity splitting is caused by the f-f transfer term.

§ 7. Summary

We reviewed a method to calculate the excitation spectra of the impurity

Anderson model on the basis of the NRG technique.

It was applied to study the SPE spectrum of the Anderson model in wide energy range for the cases of various magnitudes of the f-f Coulomb interaction. It was shown that the main peak of the SPE is always narrowed by the f-f interaction and tends gradually to the Kondo resonance. The width of the peak is always comparable to the energy scale of the magnetic excitation. These facts indicate difficulty to interpret the broad PES-BIS spectrum of U-compounds by the usual impurity Anderson model with constant f-f Coulomb interaction. Multiplet splitting of atomic states seems to be important.

The dynamical excitation spectra of low energy region were studied. They tend to a universal shape when U increases by fixing the occupation number of f-electron and energy is scaled by T_K. Tails of the SPE spectrum have much larger intensity than those given by the simple Lorentzian shape. The magnetic excitation is reproduced rather well by the RPA-like expression in which the hybridization width and the f-f interaction constant are replaced by effective ones.

The Kondo effect due to ions with Sm- and Tm- like multiplet structure was studied. Cross over from the electron to the hole binding types appears when the excitation energy of the magnetic multiplet, ΔE, decreases in Sm^{2+}-like configuration. In actual case of Sm ion, the hole binding type is expected in agreement with experiment of thermopower when Sm^{3+} configuration is primarily stable. The Kondo singlet in Tm^{3+} stable side is given as the two electron binding type.

The two impurity Anderson model was also studied. The low energy scale of the system is given approximately as $\omega_l \sim T_K\{((j-j_c)/1.5)^2+(t/23T_K)^2\}$ near the region where the cross over from the Kondo singlet like to the local-spin-singlet like states occurs. The γ-coefficient is given approximately as ω_l^{-1}, while the antiferromagnetic susceptibility as $-\ln\omega_l$. The cross over becomes singular when the f-f transfer, t, is zero and thus the terms causing parity splitting are dropped.

Calculation of excitation spectra based on the NRG technique seems to be a useful method to study the strongly correlated systems.

Acknowledgements

It is a great pleasure for two of authors (O.S. and Y. S.) to collaborate with Professor T. Kasuya on the occasion of his retirement from Tohoku University. The authors would like to thank H. Shiba for stimulating discussions, and to T. Saso and Y. Kuramoto for enlightening discussions. This work has been partly supported by the Grant-in Aids No. 02216101 and No. 03247105 from the Ministry of Education, Science and Culture. The numerical computation was partly performed at the Computer Center of Institute for Molecular Science.

References

1) K. G. Wilson, Rev. Mod. Phys. **47** (1975), 773.
2) H. R. Krishna-murthy, J. W. Wilkins and K. G. Wilson, Phys. Rev. **B21** (1980), 1003, 1044.
3) O. Sakai, Y. Shimizu and T. Kasuya, J. Phys. Soc. Jpn. **58** (1989), 3666.

4) O. Sakai, Y. Shimizu, R. Takayama and T. Kasuya, Physica **B163** (1990), 695.
5) Y. Shimizu, O. Sakai and T. Kasuya, submitted to J. Phys. Soc. Jpn.
6) Y. Shimizu, O. Sakai and T. Kasuya, Physica **B163** (1990), 401.
7) O. Sakai, Y. Shimizu and T. Kasuya, Solid State Commun. **75** (1990), 81.
8) O. Sakai and Y. Shimizu, submitted to J. Phys. Soc. Jpn.
9) In this process, the re-orthogonalization of bases is necessary to avoid numerical instability, Y. Shirono, Master Thesis of Tohoku University (1990), (unpublished).
10) In Eq. (4) of Ref. 3), the sign factor should be replaced by $(-1)^{n_i+j_i+j'_{i-1}+J_i}$ and in Eq. (7) by $(-1)^{n_i+j_i+j_i+J_i+J'_{i-1}}$.
11) H. O. Frota and L. N. Oliveira, Phys. Rev. **B33** (1986), 7871.
12) M. Yoshida, M. A. Whitaker and L. N. Oliveira, Phys. Rev. **B41** (1990), 9403.
13) See for example, A. Yoshimori and A. Zawadowski, J. of Phys. **C15** (1982), 5241.
14) H. Shiba, Prog. Theor. Phys. **54** (1975), 967.
15) See for example, O. Gunnarsson and K. Schönhammer, *Handbook on the Physics and Chemistry of Rare Earths*, ed. K. A. Gschneidner, Jr., L. Eyring and S. Hüfner (North-Holland, 1987), vol. 10, p. 103.
16) Y. Baer, *Handbook on the Physics and Chemistry of the Actinides*, ed. A. J. Freeman and G. H. Lander (North-Holland, 1984), vol. 1, p. 271.
17) H. R. Ott and Z. Fisk, *Handbook on the Physics and Chemistry of the Actinides*, ed. A. J. Freeman and G. H. Lander (North-Holland, 1987), vol. 5, p. 85.
18) C. Laubschat, W. Gerntz and G. Kaindl, Phys. Rev. **B37** (1988), 8082.
19) T. Ejima, Master Thesis of Tohoku University (1991), (unpublished).
20) J. W. Allen, S. -J. Oh, L. E. Cox, W. P. Ellis, M. S. Wire, Z. Fisk, J. L. Smith, B. B. Pate, I. Lindau and A. J. Arko, Phys. Rev. Lett. **54** (1985), 2635.
21) A. J. Arko, C. G. Olson, D. M. Wieliczka, Z. Fisk and J. L. Smith, Phys. Rev. Lett. **53** (1984), 2050.
22) See for example, A. Kotani and T. Yamazaki, Prog. Theor. Phys. Suppl. No. 108 (1992), 117.
23) J. S. Kang, J. W. Allen, M. B. Maple, M. S. Torikachvili, B. Pate, W. Ellis and I. Lindau, Phys. Rev. Lett. **59** (1987), 493.
24) D. D. Sarma, S. Krummacher, A. Wallash and J. E. Craw, Phys. Rev. **B34** (1986), 3737.
25) S. Takagi, private communication.
26) Y. Kuramoto, Z. Phys. **B53** (1983), 37.
27) O. Gunnarsson and K. Schönhammer, Phys. Rev. **B28** (1983), 4315; **B31** (1985), 4815.
28) O. Sakai, M. Motizuki and T. Kasuya, *Core-Level Spectroscopy in Condensed Systems*, ed. J. Kanamori and A. Kotani (Springer-Verlag, 1988), p. 45.
29) See for example, A. Okiji and N. Kawakami, *Theory of Heavy Fermion Systems and Valence Fluctuations*, ed. T. Kasuya and T. Saso (Springer-Verlag, 1985), p. 46, p. 57.
30) K. Yamada, Prog. Theor. Phys. **53** (1975), 970.
K. Yosida and K. Yamada, ibid. 1286.
31) See for example, N. E. Bickers, Rev. Mod. Phys. **59** (1987), 845.
32) Similar expression has been proposed by Y. Kuramoto and K. Miyake, J. Phys. Soc. Jpn. **59** (1990), 2831.
33) E. Umlauf, P. Sütsch and E. Hess, *Crystalline Electric Field and Structural Effects in f-Electron Systems*, ed. J. E. Craw, R. P. Guertin and T. W. Mihalisin (Plenum, 1980), p. 341.
34) See for example, T. Saso, Prog. Theor. Phys. Suppl. No. 108 (1992), 89.
35) See for example, B. A. Jones, *Field Theories in Condensed Matter Physics*, ed. Z. Tesanovic (Addison-Wesley, 1990), p. 87.
36) B. A. Jones, C. M. Varma and J. W. Wilkins, Phys. Rev. Lett. **61** (1988), 125.
37) See for example, J. Rossat-Mignod, L. P. Regnault, J. L. Jacoud, C. Vettier, P. Lejay, J. Flouquet, E. Walker, D. Jaccard and A. Amato, J. Magn. Magn. Mater. **76&77** (1988), 376.
38) See for example, K. Miyake, J. Magn. Magn. Mater. **63&64** (1987), 411.
39) K. Yamada, Prog. Theor. Phys. **62** (1979), 901.
40) Y. Ono, T. Matsuura and Y. Kuroda, Physica **C159** (1989), 873.
41) C. -I. Kim, Y. Kuramoto and T. Kasuya, J. Phys. Soc. Jpn. **59** (1990), 2414.
42) T. Koyama and M. Tachiki, Phys. Rev. **B36** (1987), 437.